ARTICLE
Journal of Cellular Biochemistry 115:1299–1307 (2014)

Journal of Cellular Biochemistry

# ROCK-2 Is Associated With Focal Adhesion Maturation During Myoblast Migration

K.P. Goetsch,[1] C. Snyman,[1] K.H. Myburgh,[2] and C.U. Niesler[1]*

[1]*Discipline of Biochemistry, School of Life Sciences, University of KwaZulu-Natal, Pietermaritzburg, South Africa*

[2]*Department of Physiological Sciences, University of Stellenbosch, Stellenbosch, South Africa*

## ABSTRACT

Satellite cell migration is critical for skeletal muscle growth and regeneration. Controlled cell migration is dependent on the formation of mature focal adhesions between the cell and the underlying extracellular matrix (ECM). These cell–ECM interactions trigger the activation of signalling events such as the Rho/ROCK pathway. We have previously identified a specific role for ROCK-2 during myoblast migration. In this study we report that ROCK inhibition with Y-27632 increases C2C12 myoblast velocity, but at the expense of directional migration. In response to Y-27632 an increased number of smaller focal adhesions were distributed across adhesion sites that in turn were clearly larger than sites in untreated cells, suggesting a reduction in focal adhesion maturation. We also confirm ROCK-2 localisation to the focal adhesion sites in migrating myoblasts and demonstrate a change in the distribution of these ROCK-2 containing adhesions in response to Y-27632. Taken together, our observations provide further proof that ROCK-2 regulates directional myoblast migration through focal adhesion formation and maturation. J. Cell. Biochem. 115: 1299–1307, 2014. 

**KEY WORDS:** MYOBLAST MIGRATION; Rho-KINASE\ROCK; FOCAL ADHESIONS; WOUND REPAIR

Controlled cell migration, facilitated through cell–cell and cell–substrate interactions, is essential for tissue formation, wound repair, and cellular maintenance [Friedl and Wolf, 2010]. Migration is regulated through the coordination of multiple cellular events including polarisation, cytoskeletal reorganisation, membrane turnover, cell adhesion remodelling, and cell body contraction and retraction [Amano et al., 2010]. Each cell type enables migration in response to the distinct molecular and extracellular substrate-based guidance cues it encounters that are interpreted through receptors. Subsequent adaptations of the cytoskeleton alter the morphology of the cell through changes in the development of protrusions (i.e. lamellipodia or fillipodia) that in turn facilitate cellular motility [Yamada et al., 2003; Paluch et al., 2006].

Attachment of cells to the substratum or ECM is regulated via a range of cell–matrix adhesion proteins, including integrins and subsequent modulation of signal transduction [Dhawan and Helfman, 2004]. In response to mechanical tension, as is created during wounding, integrins are clustered at the leading front. Cytoplasmic scaffold proteins such as actin-binding proteins talin and vinculin are recruited and associate with the integrin cytoplasmic tails to hold individual adhesions in early focal clusters. Focal adhesion maturation continues as these clusters subsequently aggregate into dense focal adhesions that serve as traction points during migration. Through the integrin–vinculin axis a physical link is established between the ECM and the cytoskeleton that translates substrate binding to cell motility [Tadokoro et al., 2003; Hintermann and Quaranta, 2004] subsequent myosin-II cross-linking and stress fibre contraction allows forward migration [Chrzanowska-Wodnicka and Burridge, 1996; Gilbert et al., 2010; Wehrle-Haller, 2012; Stricker et al., 2013].

Small Rho GTPases are molecular switches that control actin cytoskeleton organisation and thereby contractile responses as required during cell adhesion and migration [Nakagawa et al., 1996; Etienne-Manneville and Hall, 2002]. Rho-associated kinase (ROCK), an effector of the small GTPase Rho, is a serine/threonine kinase that promotes actin-myosin mediated contractile force generation through the phosphorylation of at least three downstream target proteins [Leung et al., 1996]. Firstly it phosphorylates LIM kinase 1 and 2 (LIMK-1 and LIMK-2) at conserved threonines in their activation loops, increasing LIMK activity. This leads to cofilin

K.P. Goetsch and C. Snyman contributed equally to this work.

Grant sponsor: South African National Research Foundation; Grant sponsor: Technology Innovation Agency; Grant sponsor: University of KwaZulu-Natal.

*Correspondence to: Dr. C. U. Niesler, Discipline of Biochemistry, School of Life Sciences, University of KwaZulu-Natal, Pietermaritzburg, South Africa. E-mail: carolaniesler@gmail.com

Manuscript Received: 9 December 2013; Manuscript Accepted: 6 February 2014

Accepted manuscript online in Wiley Online Library (wileyonlinelibrary.com): 12 February 2014

DOI 10.1002/jcb.24784 • © 2014 Wiley Periodicals, Inc.

protein inactivation via phosphorylation, preventing F-actin severing and resulting in increased stress fibre formation (Scott and Olson, 2007). ROCK also directly phosphorylates myosin light chain (MLC) as well as the myosin binding subunit (MYPT1) of the MLC phosphatase to inhibit its catalytic activity. These factors all induce stress fibre formation and focal adhesion assembly [Totsukawa et al., 2000; Riento and Ridley, 2003; Yoneda et al., 2005]. ROCK activation therefore leads to a concerted series of events that promote force generation and related morphological changes, contributing directly to actin-myosin mediated processes, such as motility, adhesion, contraction and retraction [Holtje et al., 2005; Olson, 2008; Amano et al., 2010].

ROCK exists in two isoforms, ROCK-1 (ROKβ) and ROCK-2 (ROKα). These isoforms share a 64% amino acid sequence identities [Amano et al., 2010] with both proteins expressed in most mammalian tissues. However, ROCK-2 has been identified at higher concentrations in the brain and muscle, whereas ROCK-1 was found to be prominent in non-neural tissues including the liver, lungs and testis [Leung et al., 1996; Nakagawa et al., 1996]. Several differences in activation and cellular function between these isoforms have also been identified. Specifically ROCK-1 is known to be cleaved via caspase-3 activity and ROCK-2 by granzyme B [Coleman et al., 2001]. ROCK-1 inactivation has been linked to terminal fusion of myoblasts [Nishiyama et al., 2004], whereas ROCK-2 has been suggested to be the dominant isoform required for myoblast migration, however, their roles differ across cell types and are specific to external guidance cues from the substrate [Yamada et al., 2003; Pelosi et al., 2007; Goetsch et al., 2011]. Gene expression has also suggested different cellular functions of these two proteins; ROCK-1 has been implicated in stress fibre formation in fibroblasts [Yoneda et al., 2005] and ROCK-2 appears necessary for phagocytosis and cell contraction in smooth muscle cells [Wang et al., 2009]. However, the specific function of each ROCK isoform within skeletal muscle remains largely unclear.

In this study, we analysed the role of ROCK signalling during myoblast migration and investigated the importance of ROCK during focal adhesion assembly. In order to investigate the functional effects of ROCK, we employed the use of the cell permeable ROCK inhibitor, Y-27632 [Shimokawa and Rashid, 2007]. Y-27632 has been broadly used as a highly specific Rho-kinase inhibitor as it causes an induced-fit conformational change to increase contacts with the Rho-kinase phosphate loop, which may account for its specificity [Ishizaki et al., 2000; Narumiya et al., 2000; Olson, 2008]. We provide evidence that, although ROCK inhibition accelerates myoblast migration in vitro, it does this at the expense of directionality. Importantly, our data also underscores the importance of ROCK in focal adhesion maturation and cell morphology during migration and furthermore implicates the ROCK-2 isoform as a key facilitator during skeletal muscle stem cell migration.

## MATERIALS AND METHODS

### CELL CULTURE

The C2C12 murine cell line was kindly donated by the Cape Heart Center, University of Cape Town, South Africa. Growth media consisted of Dulbecco's Modified Eagle Medium (DMEM, Highveld Biological, CN3193-9), L-glutamine (2% v/v, Cambrex, 17-605E), PenStrep (2% v/v, Cambrex, 17-602E) and Foetal calf serum (10% v/v, Invitrogen, 10108165). All cell culture was carried out under sterile conditions in a level II biological safety cabinet (ESCO class II BSC) and incubated in a $CO_2$ incubator (Innova CO-170) at 37°C, 5% $CO_2$. The culture medium was changed every 2 days. After reaching 80% confluence, cells were detached with 0.25% trypsin/1 mM EDTA (Cambrex, 17-161E) and sub-cultured in T75 flasks.

### SCRATCH ASSAY

The scratch assay was adapted from Goetsch and Niesler [2011]. Briefly, for brightfield microscopy analysis, C2C12 myoblasts were cultured to 80% confluence in 24-well plates. A scratch was made using a sterile pipette tip and the percentage wound closure was assessed over a period of 5 h in the presence or absence of the ROCK inhibitor, Y-27632 (10 μM; Calbiochem, 688001) [Alvarez et al., 2008; Xu et al., 2012]. Wounds were photographed at hours 0, 3 and 5 with a Motic 3 megapixel camera linked to an Olympus CKX41 inverted microscope (4× objective). The areas along the border of the wounds at each time point were traced using the Motic 2.0 image analysis software and the wound closure calculated as a percentage of the original wound size. The rate of migration was calculated as the percentage wound closure gradient over 5 h for three independent experiments.

### LIVE CELL TRACKING

Cells were seeded onto a 3 cm glass-bottom tissue culture dish (Matek Corporation, *P35G-1.5-14-C*) and the scratch assay was performed as previously described. Cells were either untreated (control) or treated with 10 μM Y-27632. Real-time visualisation was achieved by differential interference contrast (DIC) microscopy, utilizing the Zeiss LSM 710 confocal microscope, within an incubated chamber (37°C, 5% $CO_2$). Images were taken at 2 min intervals for 5 h. Live cell analysis was done by tracking the paths of seven individual cells per treatment group using the manual cell tracker plug-in for ImageJ (available as freeware at rsbweb.nih.gov/ij/). Cell displacement from the wound edge was plotted with the chemotaxis ImageJ plug-in. Changes in the morphology of untreated and treated cells were illustrated by overlaying the outlines of representative cells collected at 8 time points over a assay period.

### CHEMOTAXIS ASSAY

A 2D chemotactic assay chamber (iBidi) was seeded with C2C12 myoblasts ($3 \times 10^6$ cells/ml) and incubated for 4 h to allow for cell attachment. Cells were subsequently either treated with Y-27632 (10 μM) or left untreated for 20 min. An exogenous gradient of human hepatocyte growth factor (hHGF; Preprotech, 100-39), at a final concentration of 100 ng/ml, was then applied to the top chamber. This gradient has been shown to be stable for up to 48 h post-application [Suraneni et al., 2012]. Cells were further cultured within an incubated chamber unit (37°C, 5% $CO_2$) of the Zeiss 710 LSM confocal microscope and DIC images were captured every 10 min for 16 h with the 10× objective. Images were analysed with the iBidi Chemotaxis and Migration Tool 2.0 software. The

trajectories of 40 migrating cells were plotted (per treatment) and represented as rose diagrams to indicate directional integrity. The accumulated distance, forward migration index (FMI) and cellular velocity was also calculated.

### IMMUNOFLUORESCENCE STAINING

C2C12 cells were cultured to 80% confluence in 24-well plates on coverslips. Cultures were wounded as per the scratch assay and treated with 10 μM Y-27632 for a 5 h period or left untreated (control). Cells were washed with PBS, fixed in a 4% paraformaldehyde solution, incubated in blocking solution (5% donkey serum in PBS buffer (pH 7.4)) for 1 h and then immunolabelled using primary antibodies to ROCK-2 (1/1,000, polyclonal goat anti-rat ROCK-2, Santa Cruz, Sc-1851) and vinculin (1/1,000, monoclonal mouse anti-human vinculin, Sigma, V9131) for 4 h at room temperature. Cells were then washed with PBS and incubated (room temperature) with secondary antibodies, Dylight 594-conjugated donkey anti-goat IgG (1/800, Jackson Scientific) and Dylight 488-conjugated donkey anti-mouse IgG(1/800, Jackson Scientific) for 1 h. The actin cytoskeleton was visualised with TRITC-conjugated phalloidin (1/20,000, Sigma, P1951) which was added with the secondary antibody. Nuclei were visualised with Hoechst (1/4,000, Sigma, B2261) for 5 min. Coverslips were washed, mounted with Moviol and viewed with the Zeiss 710 confocal microscope. Recorded images were processed with Zen 2010 software for intensity profiles across adhesion sites. Size and number of vinculin-positive adhesions within focal adhesion sites was assessed with the Threshold plug-in for ImageJ. Segmentation settings were adjusted to optimise visualisation of vinculin labelling and particles bigger than a minimum size were automatically counted.

### WESTERN BLOT ANALYSIS

Cells were cultured until 80% confluent in T75 flasks. Cell cultures were untreated or treated with Y-27632. Lysates were harvested 4 h post-treatment using RIPA buffer (Sigma, pH 8) and a protease inhibitor cocktail (Sigma, P8340). Proteins (25 μg) were separated on a 10% SDS–PAGE gel and transferred to nitrocellulose. Blots were probed separately using monoclonal mouse anti-human vinculin IgG (1/1,000) and a polyclonal goat anti-rat ROCK-2 antibody (1/2,000). The polyclonal rabbit anti-human GAPDH primary antibody (1/4,000, Cell Signaling, 2118) was utilised as the internal loading control. An HRP-conjugated donkey anti-goat secondary antibody (1/20,000, Santa Cruz, Sc-5286) was used to detect ROCK-2, and an HRP-conjugated rabbit anti-mouse secondary antibody (1/16,000, Dako, P0260) was used to detect GAPDH and vinculin. Enhanced chemiluminescence (ECL) was used to visualise protein expression (Immun-Star WesternC, BioRad). Densitometry analysis was carried out using Quantity One 2.6 (BioRad).

### STATISTICAL ANALYSIS

For the scratch assay, six independent experimental data sets were obtained for each treatment or substrate. Data were determined to be non-parametric. The Mann–Whitney *U*-test was therefore used to calculate *P*-values for the differences between the means of experimental conditions and control. The Rayleigh test for vector data was used to assess the significance of the chemotactic effect. Image quantification and blot analysis was performed in duplicate for three independent experiments and the Student's *t*-test was utilised for statistical analysis. *Genstat* was used for all statistical tests and significance was determined as $P < 0.05$. Results are presented as the mean ± the standard error of the mean (SEM).

## RESULTS

### ROCK INHIBITOR Y-27632 ACCELERATES C2C12 MYOBLAST MIGRATION

We hypothesised that ROCK may regulate myoblast migration during wound repair due to its role in cytoskeletal reorganisation. We therefore performed a scratch assay comparing the effect of Y-27632 treatment versus growth media control on wound closure. Y-27632 treatment significantly increased the percentage wound closure compared with the untreated control at 5 h post-wounding by 21.94% (Fig. 1A). This was also reflected in the rate of migration over 5 h with a significant 1.5-fold increase following Y-27632 treatment compared to the untreated control (Fig. 1B). Scratch assay experiments were analysed up to 5 h to reduce the influence of proliferation and a possible decrease in motility due to confluence at complete wound closure. Analysis of trajectories from live cell microscopy revealed an increase in the overall displacement of Y-27632-treated cells from the wound edge into the cleared area compared to control (Fig. 1C,D). These data suggest a general restraining role of ROCK during myoblast migration.

### ROCK REGULATES DIRECTIONAL MIGRATION AND VELOCITY OF HGF-STIMULATED MYOBLASTS

We next assessed whether ROCK plays a role in maintaining directional motility of migrating myoblasts. The iBidi chamber allows free cell migration in a 360° field and maintains a stable chemotactic gradient for up to 48 h. HGF is a key activator and regulator of myoblast motility during wound repair [Griffin et al., 2010] cells were therefore induced to migrate towards the HGF chemotactic gradient applied within the iBidi chemotaxis chamber system. The cells migrated successfully for the duration of the experiment (16 h) (Fig. 2A). Directional data trajectories summarised in circular "rose" plot histograms revealed a clear chemotactic gradient towards HGF in the control cells (Fig. 2B). However, when cells were treated with Y-27632, directional cell migration was lost, with cells moving in a random configuration (Fig. 2C). Statistical analysis of this data using the *Rayleigh test* confirmed a significant chemotactic effect for the untreated control ($P < 0.000291$), which was lost on treatment with Y-27632 ($P < 0.675$). This was confirmed by the significantly greater forward migration index (FMI) along the HGF chemotactic gradient of the control cells compared to Y-27632 treated myoblasts (Fig. 2D). The Euclidean distance (shortest distance between start and end of migration) for untreated versus treated groups was similar (Supplementary Fig. 1), whereas the accumulated distance travelled increased significantly with Y-27632 treatment, compared to the untreated control (Fig. 2E). This coincided with a change in cellular velocity, which increased significantly following Y-27632 treatment (Fig. 2F). Together these data indicate a greater distance travelled by

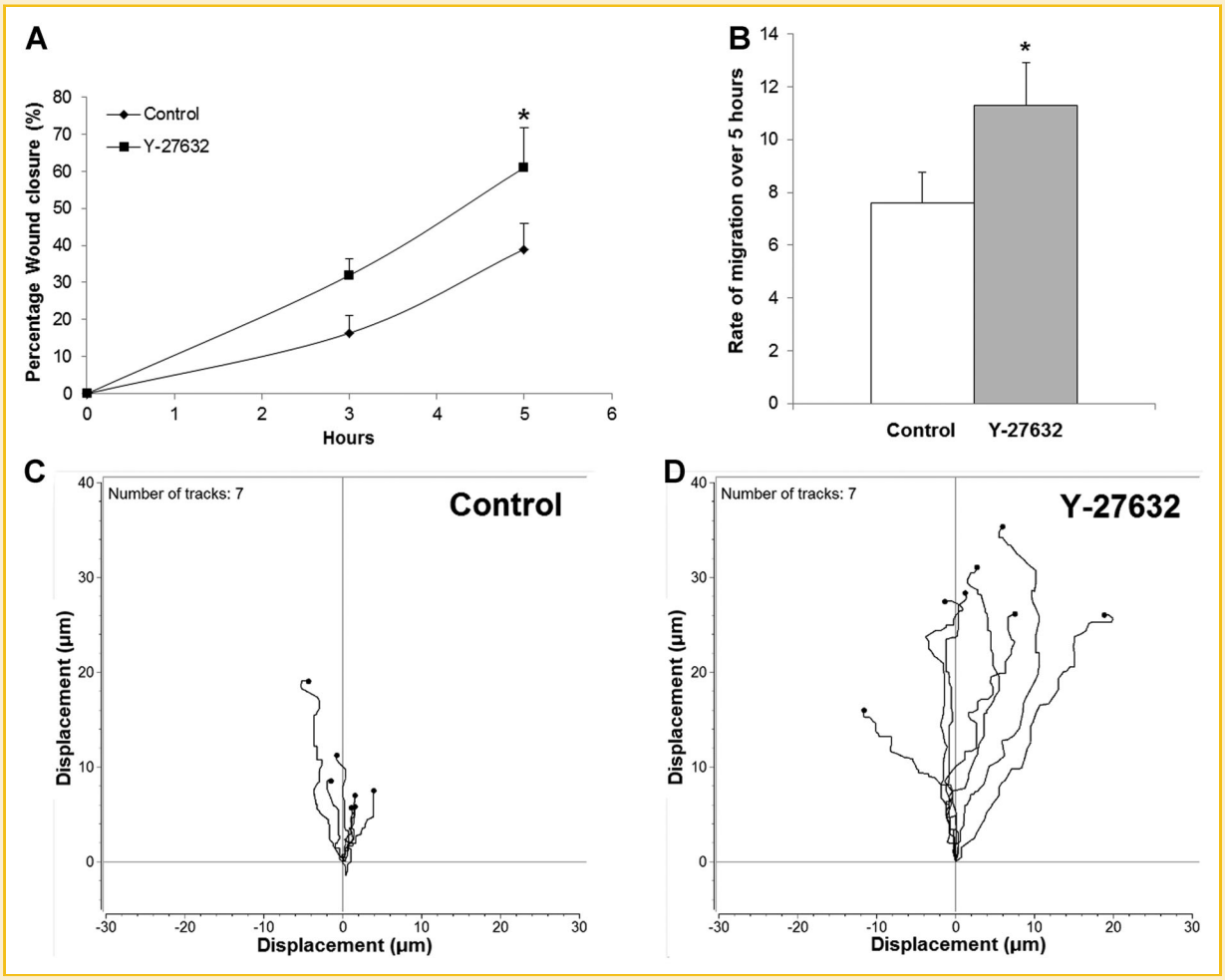


**Fig. 1.** ROCK inhibition increases rate of myoblast migration during wound repair. A: A 5 h scratch assay was performed with images captured at hours 0, 3 and 5. The percentage wound closure was calculated with the Motic 2.0 software. B: The rate of migration over 5 h. C,D: Live-cell tracking of C2C12 myoblasts over a 5 h scratch assay monitored via phase-contrast microscopy within an incubated viewing chamber. Seven cells along the leading front were tracked using ImageJ (manual tracking plugin). Displacement, from original starting position, was determined for the untreated control group (C) and the Y-27632-treated group (D). Data are mean values ± SEM for at least three independent experiments. $^*P < 0.05$.

Y-27632-treated cells and an increased migration velocity, but at the expense of regulated directional migration towards a chemotactic gradient, in this case HGF. Such altered velocity and lack of directionality are clear indications of a loss of the cells' ability to interpret external signalling cues following ROCK inhibition. This could have implications for the ability of myoblasts to reach their target area if ROCK inhibitors were to be used as pharmacological agents in an in vivo setting. These data also confirm our previous observations and suggest a role for ROCK in regulating directional migration of skeletal muscle myoblasts.

### Y-27632 ALTERS MYOBLAST MORPHOLOGY DURING WOUND REPAIR

Y-27632 was observed to affect myoblast morphology during wound repair, as shown by the change in cell shape over time and the assessment of cellular trajectories and protrusions. Untreated myoblasts displayed relatively even rounded morphology and maintained a clear anterior–posterior cellular polarity during migration (Fig. 3A) with constant, even extension of a broad lamellipodium at the cell front and retraction of the cellular tail (Fig. 3C). Following treatment with Y-27632, myoblasts displayed a more compact cell body with an increased number of longer cellular protrusions rather than single broad lamellipodia (Fig. 3B), while retraction of the tail was strained (Fig. 3D).

### ROCK INHIBITION ALTERS THE NUMBER AND SIZE OF FOCAL ADHESIONS IN MIGRATING MYOBLASTS

We have shown that Y-27632 affects myoblast mobility, directionality and cell morphology. As the activated satellite cell interprets the surrounding extracellular cues through focal adhesions, we next assessed the effect of ROCK inhibition on focal adhesion dynamics via vinculin distribution and expression. Migrating myoblasts

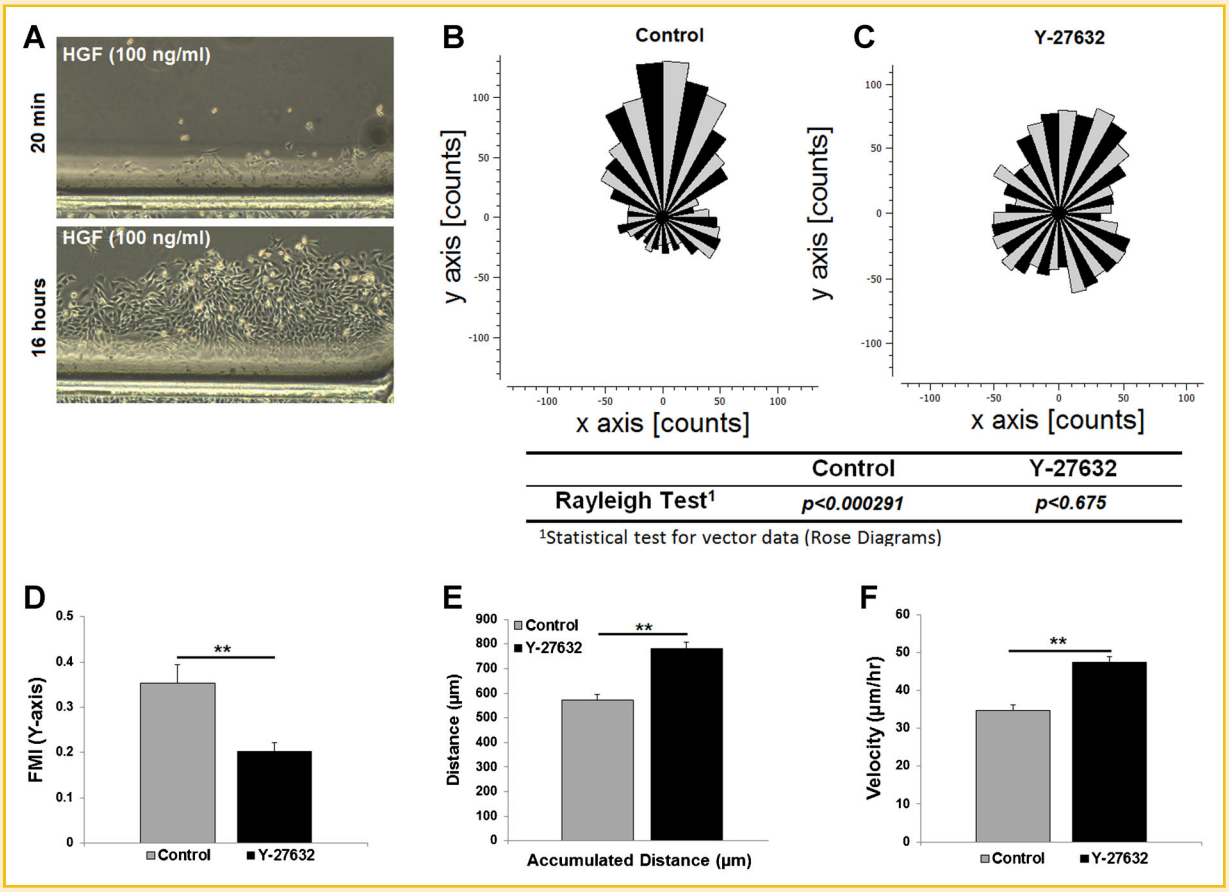


**Fig. 2.** ROCK is crucial for directional migration of C2C12 myoblasts. The 2D chemotaxis assay from iBidi was utilised to assess directional C2C12 migration. HGF, at a final concentration of 100 ng/ml, was used as chemotactic stimulus for all experimental groups. A: C2C12 myoblasts were seeded 4 h prior to treatment and subsequently treated with Y-27632 or left untreated. Cells were incubated for 20 min prior to the application of the HGF chemotactic gradient. Phase-contrast images are shown at the start (0 h) and end (16 h) of the experimental period. B,C: Rose plot diagrams representing vector-based directionality profiles for untreated and Y-27632-treated cells. The chemotactic gradient was applied along the *y*-axis and 40 cells assessed per treatment. The Rayleigh test was used for statistical analysis of all vector data. D: Forward migration index (FMI) for untreated and Y-27632-treated groups. E: Bar graph representing accumulated distance for untreated and Y-27632-treated cells. F: Velocity of C2C12 myoblasts over 16 h. The FMI and cell velocity were determined by analysis with the iBidi cell migration software. Data are mean values ± SEM for at least three independent experiments. $^{*}P < 0.05$, $^{**}P < 0.005$.

presented an accumulation of elongated vinculin-positive adhesions within distinct adhesion sites along the leading front of migrating cells, with actin stress fibres radiating from these areas across the cell body (Fig. 4A). ROCK-2 was concentrated within these focal adhesions sites, with a distribution pattern similar to that of vinculin (Fig. 4A). This was expected as we have previously shown that ROCK-2, but not ROCK-1, is localised to focal adhesions in migrating C2C12 cells [Goetsch et al., 2011]. In response to Y-27632 treatment during a 5 h scratch assay, the profile of cellular vinculin-positive adhesions changed (Figure 4A). An increased number of smaller focal adhesions were distributed across adhesion sites that in turn were clearly larger than sites in untreated cells (Fig. 4A,B). These focal adhesion sites were located at the tips of thin protrusions in migrating cells. Focal adhesion size and number was then quantified using a threshold technique [Stroeken et al., 2006]. ROCK inhibition significantly reduced the size of adhesions compared to the untreated control ($P < 0.001$; Fig. 4C) and resulted in a significant 2-fold increase in focal adhesion number ($P < 0.017$; Fig. 4D). Together these data indicate a reduction in maturation of focal adhesions.

Analysis of total vinculin expression revealed no significant change following Y-27632 treatment (Fig. 4E). This was also the case for total ROCK-2 expression (Fig. 4F). These data suggest ROCK, and more specifically ROCK-2, regulates focal adhesion clustering into more mature focal adhesions (1–5 µm in size). Importantly, this is not due to a change in total ROCK-2 or vinculin expression, but due to a redistribution of the protein within the cell.

## DISCUSSION

Injury of adult skeletal muscle results in activation of quiescent satellite cells and their migration from their niche along the basal lamina towards the injury site. Migration into the site and

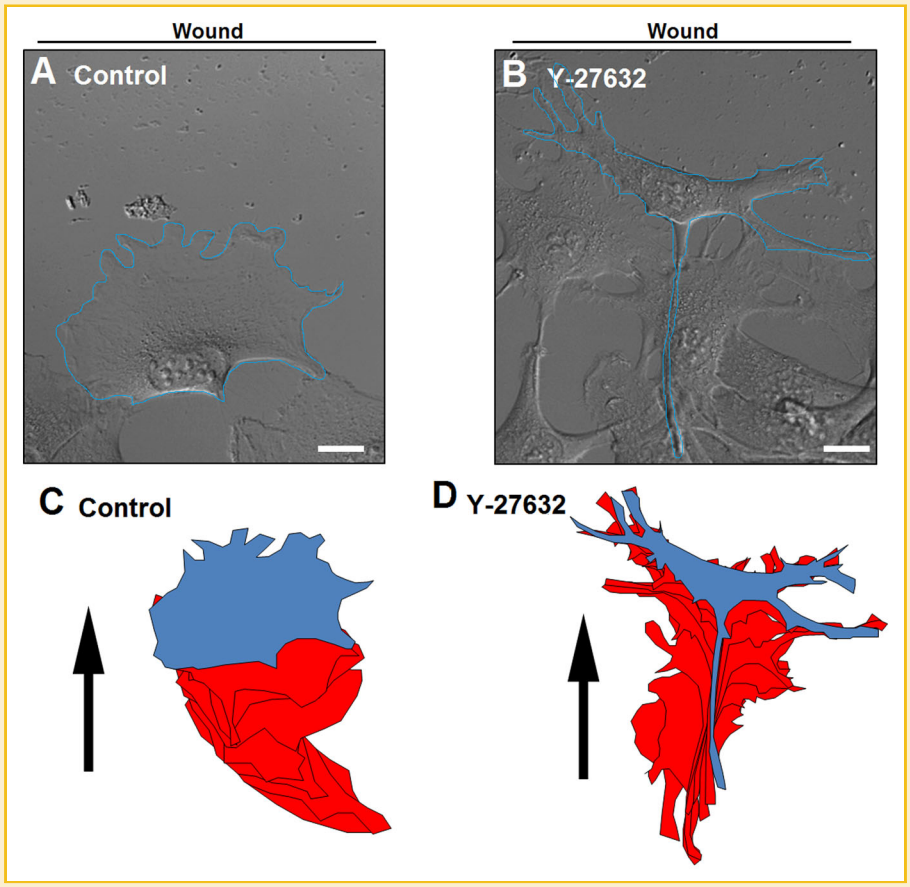


**Fig. 3.** ROCK inhibition affects C2C12 myoblast morphology during migration. Representative phase-contrast images of migrating C2C12 myoblasts at 5 h on uncoated plates, left either untreated (A) or treated with Y-27632 (10 μM) (B). Graphical representation of cell morphology changes over 5 h are shown for untreated (C) and Y-27632-treated (D) cells. Red sections represent the outline of the changing cellular morphology at 30 min intervals; arrow indicates direction of migration. Blue represents the outline of the final morphology at 5 h corresponding to the phase-contrast images. Data are of three independent experiments. Scale bar = 5 μm.

subsequent differentiation and fusion results in muscle repair [Goetsch et al., 2013]. Investigating the mechanism of satellite cell migration and the influence of the environment *en route* is essential in understanding the regeneration process and is important for the design of therapies for muscle disease and injury. Previously, we have studied the effects of injury site factors on myoblast migration and suggested that ROCK-2, rather than ROCK-1, is involved in mediating myoblast migration in general during wound repair [Goetsch et al., 2011]. In this study we focused on the migratory mechanism, examining the influence of Y-27632 on directionality and related maturation of adhesion sites.

It has been proposed, in a cancer migration study, that directional migration in epithelial cells is regulated by ROCK-2 rather than ROCK-1 [Vega et al., 2011]. Therefore we attempted to clarify the role of ROCK-2 specifically during mesenchymal C2C12 myoblast migration, as investigations looking specifically at Rho kinases within this cell model are limited. We found that incubation with Y-27632 resulted in a significant increase in the rate of myoblast migration from the wound edge into a cleared space during scratch assays, consistent with results seen in other cell-types [Kroening et al., 2010; Shum et al., 2011]. This demonstrates a restraining role of ROCK, slowing down migration in general, and suggests a possible beneficial use of ROCK inhibition during transplantation studies for effective muscle repair [Furuya et al., 2009]. However, persistence of directionality during such migration is pertinent for migration towards a wound. In contrast to scratch assays, during chemotactic assays cells are free to migrate in any direction. We found that directional migration during such chemotactic attraction was compromised with a concomitant reduction in the FMI when cells were treated with Y-27632. Similar to our initial scratch assay results Y-27632 significantly increased the accumulated distance and velocity, but the overall Euclidean distance did not change. Such lack of linear displacement and lack of directionality, despite increased velocity, are clear indications of a loss of efficiency in guided motility following ROCK inhibition. These findings emphasise that, although ROCK restrains migration, it is also important in maintaining directional migration. We propose that this positive restraint is based on interaction with external stimuli from the ECM.

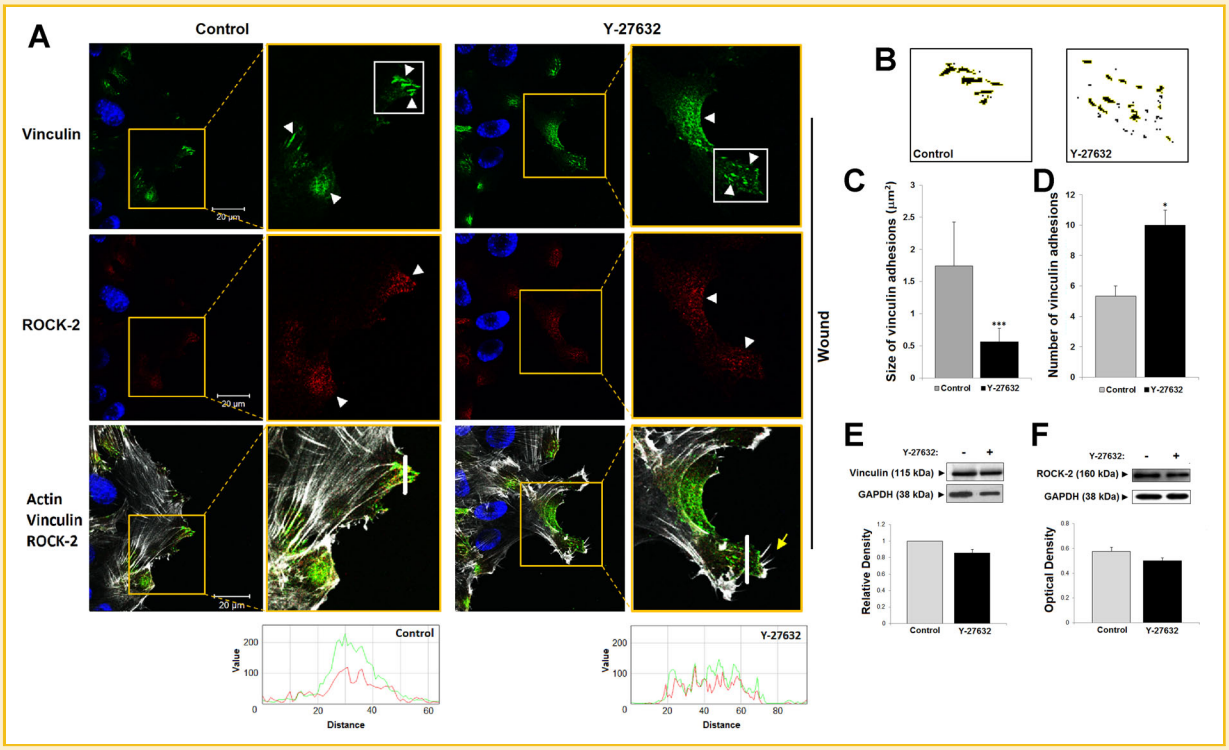


**Fig. 4.** ROCK inhibition alters focal adhesion size and number in migrating myoblasts. A: Confocal images of C2C12 myoblasts along the leading front 5 h post-wounding in the presence or absence of Y-27632 (10 μM). Focal adhesion formation assessed via vinculin localisation shown in top panel (green; white arrow heads). ROCK-2 localisation to focal adhesion sites is shown in the middle panel (red; white arrow heads). F-actin fibres, stained with phalloidin (white) merged with vinculin (green) and ROCK-2 (red) immunocytochemistry. Nuclei stained with Hoechst (blue). Filopodia formation indicated by a yellow arrow. The white line indicates the intensity profile for control and Y-27632. The green line within the intensity profile indicates vinculin, whereas the red indicates ROCK-2 intensity. Scale bar = 20 μm. B: Threshold analysis using ImageJ plugin. C&D: Adhesion size and number were assessed using ImageJ. Focal adhesion size (C) for vinculin-labelled adhesions in cells along the leading front and number of vinculin-labelled focal adhesions (D) in untreated and Y-27632-treated cells. E: Representative Western blots for vinculin and associated densitometry analysis of vinculin expression. F: Representative Western blots for ROCK-2 and associated densitometry analysis for ROCK-2 expression. GAPDH was used as the internal loading control for all densitometry analysis. Data are mean values ± SEM for at least three independent experiments. $^{*}P < 0.05$, $^{***}P < 0.001$.

It was noted that changes in cell morphology could be correlated with changes in adhesion profiles and stress fibre formation under various experimental conditions. ROCK is known to regulate cytoskeletal reorganisation [Xu et al., 2012] and therefore it was not surprising that Y-27632 resulted in a change from myoblast-like cellular morphology to stellate-like cells. This is primarily due to a loss in ability of myoblasts to retract their trailing edge, leaving a long tail behind the cells [Kolega, 1998; Alblas et al., 2001]. The increased number of protrusions at the leading front of the cell in the experimental condition, compared to the single large lamellipodium of untreated cells are also indicative of a change in the cytoskeletal formation and arrangement. This generally pointed to changes in the adhesion pattern and loss of control over the forward outflow of the cell body during migration.

To further investigate the influence of ROCK in the migratory mechanism we examined the influence of Y-27632 on the maturation of focal adhesion sites, as integrin binding of the ECM is a key regulator during myoblast migration. Force transmission from the ECM relies in part on focal adhesion scaffold proteins for the regulation of actin dynamics. Specifically, vinculin and talin form transient bonds with the actin filaments at focal adhesions. This coupling plays a key role in ECM–actin force transmission [Hu et al., 2007]. Fibroblasts derived from vinculin-knockout mice demonstrated reduced adhesion, increased motility and dynamic focal adhesion formation [Saunders et al., 2006]. Using vinculin as an indicator, the focused adhesion sites within the leading lamellipodia of migrating cells were characterised as containing many individual, strong adhesions. Under conditions of stress the initial nascent adhesions grew by recruiting scaffold proteins such as vinculin, to form focal complexes (<1 μm) that matured into focal adhesions (1–5 μm) [Gardel et al., 2010; Ciobanasu et al., 2012]. These adhesions served as nucleating points from which stress fibres (required during migration) could radiate. In the current study, ROCK inhibition reduced focal adhesion size (< 1 μm) to that similar of immature focal complexes. While vinculin expression was not reduced, altered vinculin accumulation in these areas in response to Y-27632 indicated that ROCK regulates vinculin distribution as well as the accumulation of individual adhesions within the adhesion sites into strong sites. These changes appeared to control the migration process. The increased number of small adhesions

correlated with a compromised ECM–vinculin axis and the increased motility observed due to ROCK inhibition. These results, combined with ROCK-2 localisation to the focal adhesion sites in migrating myoblasts, strongly suggest an important regulatory role for ROCK-2 during focal adhesion formation and subsequent actin-ECM coupling. Given that adhesions may affect cellular morphology, the altered shape of Y-27632-treated cells shown in this study also implies a role for ROCK in the regulation of cell adhesion.

In migrating cells, the "grip" to the substrate is provided by focal adhesions and assists in translocation of the cell body. These adhesions also serve as key signalling points for motility regulation [Alvarez et al., 2008]. Actin contractility during motility requires the activation of myosin II downstream of ROCK [Choi et al., 2008; Modulevsky et al., 2012]. This acto-myosin force generated in the lamellipodia in response to RhoA/ROCK signalling induces the maturation of focal adhesions [Chrzanowska-Wodnicka and Burridge, 1996]. Y-27632 has previously been reported to decrease cell adhesion in myoblasts by 9% [Modulevsky et al., 2012]. This was confirmed by the results of the current study. Focal adhesions are still maintained during ROCK inhibition [Grashoff et al., 2010], but it is the interference with the integrin–talin–vinculin axis that limits maturation of focal adhesions and stress fibre formation and in this process, restricts adhesion strength to the substrate [Zhang et al., 2008].

In conclusion, the localisation of ROCK-2 to focal adhesion binding sites implicates it as a key isoform involved in the regulation of myoblast motility. Furthermore, our study underscores the importance of ROCK in focal adhesion maturation and cell morphology during myoblast migration. ROCK inhibition resulted in changes in adhesion morphology and cell profile. The observation of smaller focal adhesions supports the increase in velocity of cell motility which *could* be interpreted as a "positive" response. Chemotactic regulation was, however, compromised with ROCK inhibition as shown by the loss of directionality. This demonstrates that observed "positive" responses to treatment with inhibitors such as Y-27632 should carefully be considered and interpreted with relevance to the desired functional outcome, in this case effective migration. This is important, especially in pre-clinical experiments aimed ultimately at identifying potential drug targets that could improve myoblast motility during skeletal muscle repair.

## ACKNOWLEDGEMENTS

The authors thank the UKZN Microscopy and Microanalysis Unit (Pietermaritzburg) for all their assistance.

## REFERENCES

Alblas J, Ulfman L, Hordijk P, Koenderman L. 2001. Activation of Rhoa and ROCK are essential for detachment of migrating leukocytes. Mol Biol Cell 12:2137–2145.

Alvarez B, Stroeken PJ, Edel MJ, Roos E. 2008. Integrin cytoplasmic domain-associated protein-1 (ICAP-1) promotes migration of myoblasts and affects focal adhesions. J Cell Physiol 214:474–482.

Amano M, Nakayama M, Kaibuchi K. 2010. Rho-kinase/ROCK: A key regulator of the cytoskeleton and cell polarity. Cytoskeleton (Hoboken) 67:545–554.

Choi CK, Vicente-Manzanares M, Zareno J, Whitmore LA, Mogilner A, Horwitz AR. 2008. Actin and alpha-actinin orchestrate the assembly and maturation of nascent adhesions in a myosin II motor-independent manner. Nat Cell Biol 10:1039–1050.

Chrzanowska-Wodnicka M, Burridge K. 1996. Rho-stimulated contractility drives the formation of stress fibers and focal adhesions. J Cell Biol 133:1403–1415.

Ciobanasu C, Faivre B, Le Clainche C. 2012. Actin dynamics associated with focal adhesions. Int J Cell Biol 2012:941292.

Coleman ML, Sahai EA, Yeo M, Bosch M, Dewar A, Olson MF. 2001. Membrane blebbing during apoptosis results from caspase-mediated activation of ROCK I. Nat Cell Biol 3:339–345.

Dhawan J, Helfman DM. 2004. Modulation of acto-myosin contractility in skeletal muscle myoblasts uncouples growth arrest from differentiation. J Cell Sci 117:3735–3748.

Etienne-Manneville S, Hall A. 2002. Rho GTPases in cell biology. Nature 420:629–635.

Friedl P, Wolf K. 2010. Plasticity of cell migration: A multiscale tuning model. J Cell Biol 188:11–19.

Furuya T, Hashimoto M, Koda M, Okawa A, Murata A, Takahashi K, Yamashita T, Yamazaki M. 2009. Treatment of rat spinal cord injury with a Rho-kinase inhibitor and bone marrow stromal cell transplantation. Brain Res 1295:192–202.

Gardel ML, Schneider IC, Aratyn-Schaus Y, Waterman CM. 2010. Mechanical integration of actin and adhesion dynamics in cell migration. Annu Rev Dev Biol 26:315–333.

Gilbert PM, Havenstrite KL, Magnusson KE, Sacco A, Leonardi NA, Kraft P, Nguyen NK, Thrun S, Lutolf MP, Blau HM. 2010. Substrate elasticity regulates skeletal muscle stem cell self-renewal in culture. Science 329:1078–1081.

Goetsch KP, Niesler CU. 2011. Optimization of the scratch assay for in vitro skeletal muscle wound healing analysis. Anal Biochem 411:158–160.

Goetsch KP, Kallmeyer K, Niesler CU. 2011. Decorin modulates collagen I-stimulated, but not fibronectin-stimulated, migration of C2C12 myoblasts. Matrix Biol 30:109–117.

Goetsch KP, Myburgh KH, Niesler CU. 2013. In vitro myoblast motility models: Investigating migration dynamics for the study of skeletal muscle repair. J Muscle Res Cell Motility 34:333–347.

Grashoff C, Hoffman BD, Brenner MD, Zhou R, Parsons M, Yang MT, Lean McLean, Sligar SG, Chen CS, Ha T, Schwartz MA. 2010. Measuring mechanical tension across vinculin reveals regulation of focal adhesion dynamics. Nature 466:263–266.

Griffin CA, Apponi LH, Long KK, Pavlath GK. 2010. Chemokine expression and control of muscle cell migration during myogenesis. J Cell Sci 123:3052–3060.

Hintermann E, Quaranta V. 2004. Epithelial cell motility on laminin-5: Regulation by matrix assembly, proteolysis, integrins and erbB receptors. Matrix Biol 23:75–85.

Holtje M, Hoffmann A, Hofmann F, Mucke C, Grosse G, Van Rooijen N, Kettenmann H, Just I, Ahnert-Hilger G. 2005. Role of Rho GTPase in astrocyte morphology and migratory response during in vitro wound healing. J Neurochem 95:1237–1248.

Hu K, Ji L, Applegate KT, Danuser G, Waterman-Storer CM. 2007. Differential transmission of actin motion within focal adhesions. Science 315:111–115.

Ishizaki T, Uehata M, Tamechika I, Keel J, Nonomura K, Maekawa M, Narumiya S. 2000. Pharmacological properties of Y-27632, a specific inhibitor of rho-associated kinases. Mol Pharmacol 57:976–983.

Kolega J. 1998. Fluorescent analogues of myosin II for tracking the behavior of different myosin isoforms in living cells. J Cell Biochem 68:389–401.

Kroening S, Stix J, Keller C, Streiff C, Goppelt-Struebe M. 2010. Matrix-independent stimulation of human tubular epithelial cell migration by Rho kinase inhibitors. J Cell Physiol 223:703–712.

Leung T, Chen XQ, Manser E, Lim L. 1996. The p160 RhoA-binding kinase ROK alpha is a member of a kinase family and is involved in the reorganization of the cytoskeleton. Mol Cell Biol 16:5313–5327.

Modulevsky DJ, Tremblay D, Gullekson C, Bukoreshtliev NV, Pelling AE. 2012. The physical interaction of myoblasts with the microenvironment during remodeling of the cytoarchitecture. PLoS ONE 7:e45329.

Nakagawa O, Fujisawa K, Ishizaki T, Saito Y, Nakao K, Narumiya S. 1996. ROCK-I and ROCK-II, two isoforms of Rho-associated coiled-coil forming protein serine/threonine kinase in mice. FEBS Lett 392:189–193.

Narumiya S, Ishizaki T, Uehata M. 2000. Use and properties of ROCK-specific inhibitor Y-27632. Meth Enzymol 325:273–284.

Nishiyama T, Kii I, Kudo A. 2004. Inactivation of Rho/ROCK signaling is crucial for the nuclear accumulation of FKHR and myoblast fusion. J Biol Chem 279:47311–47319.

Olson MF. 2008. Applications for ROCK kinase inhibition. Curr Opin Cell Biol 20:242–248.

Paluch E, van der Gucht J, Joanny JF, Sykes C. 2006. Deformations in actin comets from rocketing beads. Biophys J 91:3113–3122.

Pelosi L, Giacinti C, Nardis C, Borsellino G, Rizzuto E, Nicoletti C, Wannenes F, Battistini L, Rosenthal N, Molinaro M, Musaro A. 2007. Local expression of IGF-1 accelerates muscle regeneration by rapidly modulating inflammatory cytokines and chemokines. FASEB J 21:1393–1402.

Riento K, Ridley AJ. 2003. Rocks: Multifunctional kinases in cell behaviour. Nat Rev Mol Cell Biol 4:446–456.

Saunders RM, Holt MR, Jennings L, Sutton DH, Barsukov IL, Bobkov A, Liddington RC, Adamson EA, Dunn GA, Critchley DR. 2006. Role of vinculin in regulating focal adhesion turnover. Eur J Cell Biol 85:487–500.

Scott RW, Olson MF. 2007. LIM kinases: Function, regulation and association with human disease. J Mol Med (Berl) 85:555–568.

Shimokawa H, Rashid M. 2007. Development of Rho-kinase inhibitors for cardiovascular medicine. Trends Pharmacol Sci 28:296–302.

Shum MS, Pasquier E, Po'uha ST, O'Neill GM, Chaponnier C, Gunning PW, Kavallaris M. 2011. Gamma-Actin regulates cell migration and modulates the ROCK signaling pathway. FASEB J 25:4423–4433.

Stricker J, Beckham Y, Davidson MW, Gardel ML. 2013. Myosin II-mediated focal adhesion maturation is tension insensitive. PLoS ONE 8:e70652.

Stroeken PJ, Alvarez B, Van Rheenen J, Wijnands YM, Geerts D, Jalink K, Roos E. 2006. Integrin cytoplasmic domain-associated protein-1 (ICAP-1) interacts with the ROCK-I kinase at the plasma membrane. J Cell Physiol 208:620–628.

Suraneni P, Rubinstein B, Unruh JR, Durnin M, Hanein D, Li R. 2012. The Arp2/3 complex is required for lamellipodia extension and directional fibroblast cell migration. J Cell Biol 197:239–251.

Tadokoro S, Shattil SJ, Eto K, Tai V, Liddington RC, de Pereda JM, Ginsberg MH, Calderwood DA. 2003. Talin binding to integrin beta tails: A final common step in integrin activation. Science 302:103–106.

Totsukawa G, Yamakita Y, Yamashiro S, Hartshorne DJ, Sasaki Y, Matsumura F. 2000. Distinct roles of ROCK (Rho-kinase) and MLCK in spatial regulation of MLC phosphorylation for assembly of stress fibers and focal adhesions in 3T3 fibroblasts. J Cell Biol 150:797–806.

Vega FM, Fruhwirth G, Ng T, Ridley AJ. 2011. RhoA and RhoC have distinct roles in migration and invasion by acting through different targets. J Cell Biol 193:655–665.

Wang Y, Zheng XR, Riddick N, Bryden M, Baur W, Zhang X, Surks HK. 2009. ROCK isoform regulation of myosin phosphatase and contractility in vascular smooth muscle cells. Circ Res 104:531–540.

Wehrle-Haller B. 2012. Assembly and disassembly of cell matrix adhesions. Curr Opin Cell Biol 24:569–581.

Xu B, Song G, Ju Y, Li X, Song Y, Watanabe S. 2012. RhoA/ROCK, cytoskeletal dynamics, and focal adhesion kinase are required for mechanical stretch-induced tenogenic differentiation of human mesenchymal stem cells. J Cell Physiol 227:2722–2729.

Yamada T, Takezawa Y, Iwamoto H, Suzuki S, Wakabayashi K. 2003. Rigor-force producing cross-bridges in skeletal muscle fibers activated by a substoichiometric amount of ATP. Biophys J 85:1741–1753.

Yoneda A, Multhaupt HA, Couchman JR. 2005. The Rho kinases I and II regulate different aspects of myosin II activity. J Cell Biol 170:443–453.

Zhang X, Jiang G, Cai Y, Monkley SJ, Critchley DR, Sheetz MP. 2008. Talin depletion reveals independence of initial cell spreading from integrin activation and traction. Nat Cell Biol 10:1062–1068.

## SUPPORTING INFORMATION

Additional supporting information may be found in the online version of this article at the publihser's web-site.